

# Phase Transition-Induced Electrical Voltage

Yuanjie Huang<sup>1\*</sup>, Liusen Hu<sup>2</sup>

<sup>1</sup>*Mianyang, Sichun province, People's Republic of China*

<sup>2</sup>*Chinese Academy of Engineering Physics, Mianyang 621900, China*

\*Corresponding author's E-mail: [hyj201207@163.com](mailto:hyj201207@163.com)

Non-uniform phase transitions are widespread phenomena in nature. Previous conventional investigations gave pressure and temperature dependence of phase regions and phase transitions, i.e.  $P$ - $T$  phase diagrams. At interfaces of different phases, here we reveal an electrical potential named after *Haiyan Zang potential* which arises from Fermi level alterations upon phase transitions. This potential may be a key for phase transition dynamics. It can induce a strong intrinsic electric field at interfaces, and the related electrical energy may cancel interfacial energy of nucleus so that they could stably exist and grow. The induced intrinsic electric field may act as another dimension, and the conventional  $P$ - $T$  phase diagrams should be changed to be pressure-temperature-electric field ( $P$ - $T$ - $E$ ) phase diagrams. These findings that *Haiyan Zang potential* and its induced intrinsic electric field at interface may offer people new understandings on phase diagrams and phase transition dynamics.

## Introduction

Under specific pressure and temperatures, materials usually experience structural phase transition (SPT), a very common and popular phenomenon. It is a primary consideration for people to understand mechanical, electrical, optical and thermal properties of materials. During SPT, the most noticeable point may be crystalline symmetry variations which can be detected very well by X-ray diffraction (XRD) techniques. On the other hand, SPT is usually accompanied by volume alterations. For example, iron undergoes a body-centered cubic (BCC) to hexagonal (HCP) phase transition at 15 *GPa* at room temperature [1], and the volume shrinks by 0.38 *cm*<sup>3</sup>/*mol* [1]. Bismuth is subject to various SPT in temperature-pressure (*P-T*) phase diagram and is customarily utilized as a pressure calibrator for high-pressure devices [2], and its volume shrinkage for I-II and II-III SPT at room temperature can reach 4.7% and 3.4% [2, 3], respectively. Beside the commonly mentioned changes of features such as latent heat, volume changes and so on, one may ask what else will happen during SPT of materials?

On the other hand, experiments and theories indicate that melting point of nanoparticles is sensitively size-dependent and lower than that of bulk material [4, 5, 6, 7, 8, 9]. It could be given by Gibbs-Tomson equation [10, 11]

$$T_m(r) = T_m(\infty) \left( 1 - \frac{2\sigma_{ls}}{\Delta H_f \rho_s r} \right),$$
 where  $T_m(\infty)$  is bulk melting point,  $\Delta H_f$  stands for bulk latent heat of fusion, and  $\rho_s$  denotes solid phase density,  $\sigma_{ls}$  is interface energy.

The paradox lies in the fact that when solidification happens, nucleated nanoparticles can sustain and stably grow at bulk melting point which is much higher than their melting

point. Upon this, the recently found *Yuheng Zhang effect* predicts that an electrical voltage appears between two phases of materials in SPT processes [12] and this electrical voltage might be responsible for this paradox.

In this work, we addressed this question by means of first-principle calculations and examined whether the predicted electrical voltage appears or not between the new phase and original phase of materials during SPT. Further, we discuss its role in phase diagrams and phase transition dynamics, especially liquid-solid transition.

## **Results and Discussion**

As is known, for two coexistent phases at the transition point, the electrochemical potential for electrons, which is a summation of Fermi level and electric potential, should be equal to each other,

$$E_{F1} + qV_1 = E_{F2} + qV_2 \quad (1)$$

where  $q$  is electron charge,  $E_{F1}$ ,  $E_{F2}$  are Fermi levels of the phases,  $V_1$  and  $V_2$  are electrical potentials for the phases. So electron transfers happen and therefore an electrical voltage emerges, given by  $(V_2 - V_1) = (E_{F1} - E_{F2})/q$ , ensuring the electric equilibrium, *i.e.*, the same electrochemical potential for different phases.

Let us examine Fermi level alterations of bismuth during SPT by first-principle calculations. In the calculations, GGA-PBE software and pseudopotentials is utilized. The calculated results are summarized in Figure 1, which gives pressure dependence of Fermi level ( $E_F$ ) for a representative metal bismuth in different phases. Under applied pressures, bismuth is subject to a STP at 2.52 *GPa* at room temperature [3], from a rhombohedral structure with space group  $R-3m$  (I phase) [2] to a monoclinic structure

with the space group  $P4/n$  (II-phase) [16] and the volume shrinkage approaches 4.7% [2]. Correspondingly, Fermi level  $E_F$  of bismuth experiences a sudden change 0.3 eV at the transition pressure 2.52 GPa shown in Figure 1. When pressure reaches 2.69 GPa, another SPT occurs, resulting in a transformation from II-phase to a tetragonal structure with space group  $P4/n$  (III-phase) [16] accompanied by the volume shrinkage 3.4% [3]. To one's surprise, Fermi level  $E_F$  of bismuth exhibits a dramatic alteration 6 eV (see Figure 1), meaning that an electrical voltage 6 V exists between the interface of II-phase and III-phase at the transition point. The pressure dependence of Fermi level for bismuth is in agreement with its electric conductivity at room temperature, as is shown in Figure 1. The electric conductivity considerably rest with applied pressure and exhibits dramatic alterations at the SPT points.

This phenomena is very like Galvani potential, a voltage existing at contact of two different materials [17]. Both of them arise from differences in Fermi level and occurs at the contact interface. But they are distinct. The Galvani potential comes from different materials and almost does not depend on temperatures whereas the voltage in SPT result from SPT of the identical material and strongly relies on temperatures and pressures. On the other hand, SPT-voltage relation were studied for one classical metal in this work, bismuth, but of emphasized is that it is common for SPT of materials such as liquid-liquid, liquid-solid and solid-solid transitions, not restricting to the above mentioned bismuth. Here, this voltage, appearing upon phase transitions of materials, is formally named as *Haiyan Zang potential* [18]. This potential may offer a new method for people to detect SPT, and might be prior to XRD for diagnosing liquid-

liquid transitions. And the corresponding experimental setup might need to be well-designed.

Now, let us address role of *Haiyan Zang potential* in liquid-solid and solid-solid phase transitions of materials. When phase transitions happen, electron transfers may happen and therefore make the phases charged, generating *Haiyan Zang potential* and an electric field at the interfaces. It may be of paramount importance in initial processes of non-uniform phase transition, nucleation and subsequent growth. Take liquid-solid transition of materials as an example, as temperature decreases to melting point  $T_m$ , solid nanoparticles may first nucleate and grow subsequently. However, the contradiction is that melting point of these nanoparticle  $T_m(r)$  is of size dependence and usually much lower than melting point of a bulk material [4, 5, 6, 7, 8, 9], *i.e.*,  $T_m(r) < T_m$ . For instance, cohesive energy of aluminum nanoparticle is also size dependent and lower than that of liquid aluminum at the melting point [9]. When solidification initially happens, how do these solid nucleuses sustain?

To tackle this problem, assuming that the Gibbs free energy for unit volume of the liquid and solid at the phase transition temperature is  $G_l$  and  $G_s$ , respectively. Like the theoretical treatments [19, 20], the total Gibbs free energy for case (a) and (b) shown in Figure 2 is

$$G_a = G_l V \quad (2)$$

$$G_b = G_l \left[ V - \frac{4\pi}{3} r^3 \right] + (G_s + E_d) \frac{4\pi}{3} r^3 + 4\pi r^2 \sigma_{ls} - 4\pi r^2 d \frac{1}{2} \epsilon_0 \epsilon E^2 \quad (3)$$

where  $V$  is the total volume of liquid,  $r$  is the radius of solid nucleus,  $\sigma_{ls}$  is the interfacial energy of nucleus,  $E_d$  is distortion energy of solid nucleus per unit volume,  $d$  stands for

width of transition region for Fermi levels near interface shown in Figure 3 and it may be regarded as a constant for one material and might be much smaller than nucleus radius,  $E$  denotes *Haiyan Zang potential*-induced electric field at interface. So the Gibbs free energy difference  $\Delta G=G_b-G_a$  is

$$\Delta G = (G_s + E_d - G_l) \frac{4\pi}{3} r^3 + 4\pi r^2 \left( \sigma_{ls} - \frac{1}{2} \varepsilon_0 \varepsilon d E^2 \right) \quad (4)$$

Because of this equation  $q dE = \Delta E_F$ , where  $q$  is electron charge,  $d$  and  $\Delta E_F$  is Fermi level difference of this liquid and solid. The Gibbs free energy difference could be written as.

$$\Delta G = (G_s + E_d - G_l) \frac{4\pi}{3} r^3 + 4\pi r^2 \left[ \sigma_{ls} - \frac{\varepsilon_0 \varepsilon}{2d} \left( \frac{\Delta E_F}{q} \right)^2 \right] \quad (5)$$

Here it is argued and stated that the electric energy equals the interfacial energy, i.e.,

$$\sigma_{ls} = \frac{\varepsilon_0 \varepsilon}{2d} \left( \frac{\Delta E_F}{q} \right)^2 \quad (6)$$

Thus the interfacial energy is canceled, and the Gibbs free energy difference is given by  $\Delta G = (G_s + E_d - G_l) \frac{4\pi}{3} r^3$ , meaning that once supercooling occurs and  $\Delta G < 0$ , many solid nucleuses will nucleate necessarily. As for the melting point of a nucleated solid nucleus in liquid-solid transition processes, once interfacial energy is canceled, the melting point of nucleus is the bulk melting point according to Gibbs-Thomson equation [10, 11]. So, the solid nucleus can maintain and grow gradually at bulk melting point in the following concreting processes, explaining the previously mentioned paradox, as inversely verifies correctness of equation (6).

Comparing with classical theory, the largest distinction in this phase transition theory resides in the last term in Equation (3), the subtraction of electrical energy at the

interface. And the two theories give the Gibbs free energy difference shown in Figure 4. Classical theory indicates existence of a critical radius and points out vital role of thermal fluctuation, i.e., only thermally fluctuated nucleuses whose radius exceeding the critical radius could sustain and grow, otherwise they will vanish due to thermal fluctuation. However, the theory in this work argues that the critical radius may not exist and the thermal fluctuation may not be as important as thought before. This theory demonstrates that if supercooling appears and  $\Delta G < 0$  the solid nucleus will gradually nucleate and grow satisfactorily. In other words, the electric field, especially *Haiyan Zang potential*-induced intrinsic electric field, is of paramount importance and is a new dimension for the phase stability and phase transitions. So, the conventional  $P$ - $T$  phase diagrams must be expanded to pressure-temperature-electric field ( $P$ - $T$ - $E$ ) phase diagrams.

Of emphasized is that this work takes liquid-solid transition as an example, but this theory may also apply for other non-uniform phase transitions with Fermi level alterations, e.g., solid-solid phase transitions, liquid-liquid phase transitions, ferromagnetic transitions, ferroelectric transitions and so on.

## **Conclusion**

In summary, *Haiyan Zang potential*, a phase transition-induced intrinsic electrical potential at interfaces of two different phases of materials, is revealed theoretically. For effect of this potential on phase transition dynamics, its corresponding electrical energy may cancel interfacial energy of nucleuses, thereby making them stabilize and grow steadily. In view of vital role of *Haiyan Zang potential* and its induced electric field in

phase transitions, the phase diagrams for various materials should be  $P$ - $T$ - $E$  phase diagrams instead of conventional  $P$ - $T$  phase diagrams. These findings may help people understand phase transitions more in-depth.

## Reference

- [1] Jamieson, J. C. and Lawson, A. W. *X-ray diffraction studies in the 100 kbar pressure range. J. Appl. Phys.*, **33**, 776-780 (1962).
- [2] E. Yu Tonkov, E. G. Ponvatovskv, *Phase Transformations of Elements Under High Pressure*, CRC Press, Boca Raton, London, New York, Washington, D.C. p148, (2005).
- [3] Getting, I. C. *New Determination of The Bi I-II Equilibrium Pressure: A Proposed Modification to The Practical Pressure Scale. Metrologia*, **35**, 119-132(1998).
- [4] Mieko Takagi, *Electron-Diffraction Study of Liquid-Solid Transition of Thin Metal Films, J. Phys. Soc. Jap. V. 9*, No. 3, 359-363(1954).
- [5] Ph. Buffat, J-P. Borel, *Size Effect on The Melting Temperature of Gold Particles, Phys. Rev. A, V. 13*, No. 6, 2287-2298(1975).
- [6] G. L. Allen, R. A. Bayles, W. W. Gile, W. A. Jesser, *Thin Solid Films*, **144**, 297-308(1986).
- [7] S. L. Lai, J. Y. Guo, V. Petrova, G. Ramanath, L. H. Allen, *Size-Dependent Melting Properties of Small Tin Particles: Nanocalorimetric Measurements, Phys. Rev. Lett. 77*, 99-102(1996).
- [8] Hanszen, K.-J. *Z. Phys. V. 157*, No. 5, 316(1960).
- [9] Saman Alavi, Donald L. Thompson, *Molecular Dynamics Simulations of Melting of Aluminum Nanoparticles, J. Phys. Chem. A 110*, 1518-1523(2006).
- [10] Catheryn L. Jackson, Gregory B. Mckenna, *The melting behavior of organic materials confined in porous solids, J. Chem. Phys. 93*(12), 9002-9011(1990).
- [11] J. Sun, S.L. Simon, *The melting behavior of aluminum nanoparticles,*

Thermochimica Acta **463**, 32-40(2007).

[12] Yuanjie Huang, *Strain Induced Electric Effect in Materials*, *viXra*: 1803.0182 (2018).

[13] P. W. Bridgman, Compressions and Polymorphic Transitions of Seventeen Elements to 100, 000 kg/cm<sup>2</sup>, *Phys. Rev.* **60**, 351-354(1941).

[14] G. Andersson, B. Sundqvist, and G. Bäckström, A highpressure cell for electrical resistance measurements at hydrostatic pressures up to 8 GPa: Results for Bi, Ba, Ni, and Si, **65**, 3943-3950 (1989).

[15] Brugger, R. M., Bennion, R. B. and Worlton, T. G. *The Crystal Structure of Bi II at 26 kbar. Phys. Lett. A*, **24**, 714-717(1967).

[16] Blanco, E., Mexmain, J. M. and Chapron, P. *Temperature Measurements of Shock Heated Materials Using Multispectral Pyrometry: Application to Bismuth. Shock Waves*, **9**, 209-214(1999).

[17] IUPAC Gold Book, definition of Galvani potential difference.

[18] Haiyan Zang was an English teacher at Fangzi junior middle school in Weifang.

The author Yuanjie Huang is grateful for her selfless guidance and help when he fell behind in English. To express his gratitude, the voltage is named after her.

[19] Dacheng Fang, Man Yao, Jiujun Xu, Xudong Wang, *Foundation of Concretion Science* (in Chinese), First Edition, Science Press, Beijing, pp. 44-49 (2013).

[20] Zhiping Tang, *Shock-Induced Phase Transition* (in chinese), First Edition, Science Press, Beijing, pp.87-89 (2008).

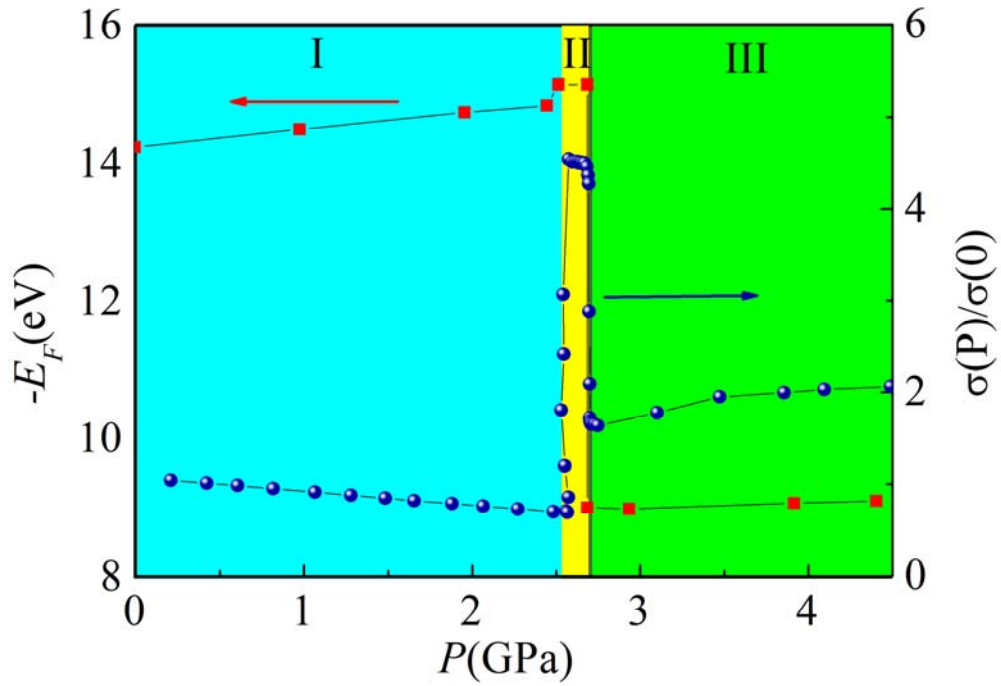


Figure 1. Pressure dependence of Fermi level and normalized electric conductivity of bismuth. Red squares, royal circles stand for Fermi level and normalized electric conductivity of bismuth at different temperatures, respectively. The Fermi level is calculated by means of first-principle calculations based on experimental data at high pressures [13] and electrical conductivity is experimental data [14]. For bismuth, I phase (cyan region) is a rhombohedral structure with space group is  $R-3m$  [2], II phase (yellow region) is a monoclinic structure with space group  $C2/m$  [15] and III phase (green region) has a tetragonal structure with space group  $P4/n$  [16], I-II and II-III phase transitions happen at  $2.52 \text{ GPa}$  and  $2.69 \text{ GPa}$  at room temperature [2, 3], respectively.

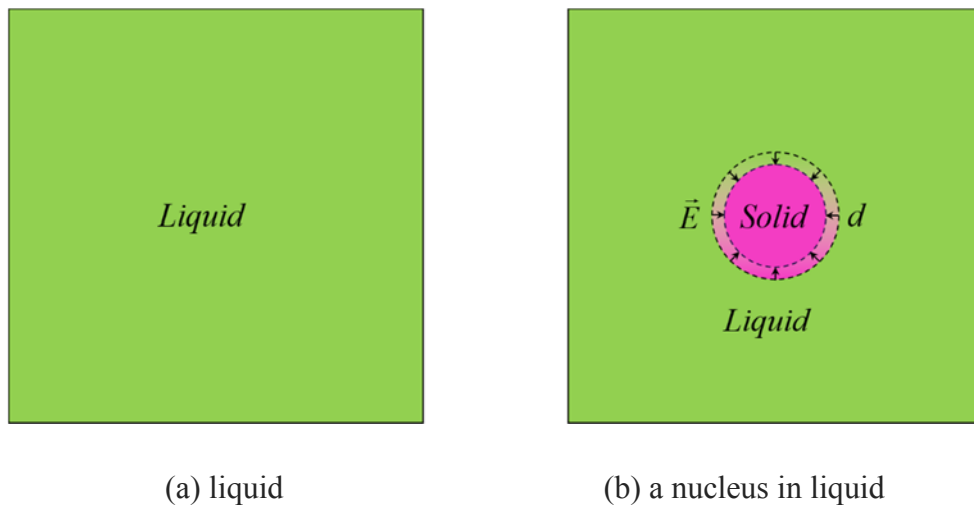


Figure 2. non-uniform liquid-solid phase transition. (a) the total volume is liquid (green zones); (b) a solid nucleus (magenta sphere) nucleates in the liquid and the liquid-solid interface (in gradual magenta) of thickness  $d$ , *Haiyan Zang potential* induced spherical electric field  $E$  is presented by black arrows.

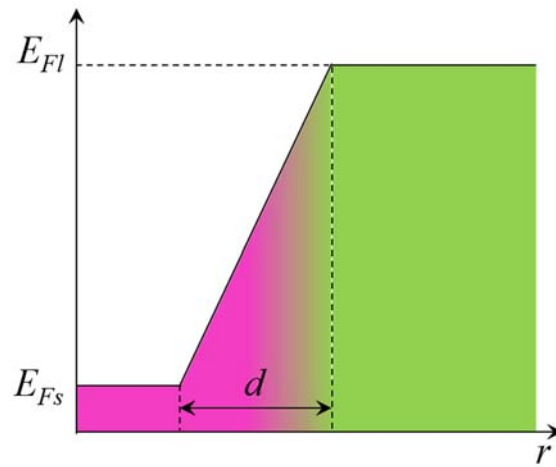


Figure 3. Schematic diagram for Fermi levels  $E_{Fs}$ ,  $E_{Fl}$  of a solid nucleus (magenta) and its surround liquid (green). The width of transition region (color gradient area) for Fermi levels is denoted by  $d$  which may be a constant for a definite material in its whole liquid-solid transition processes.

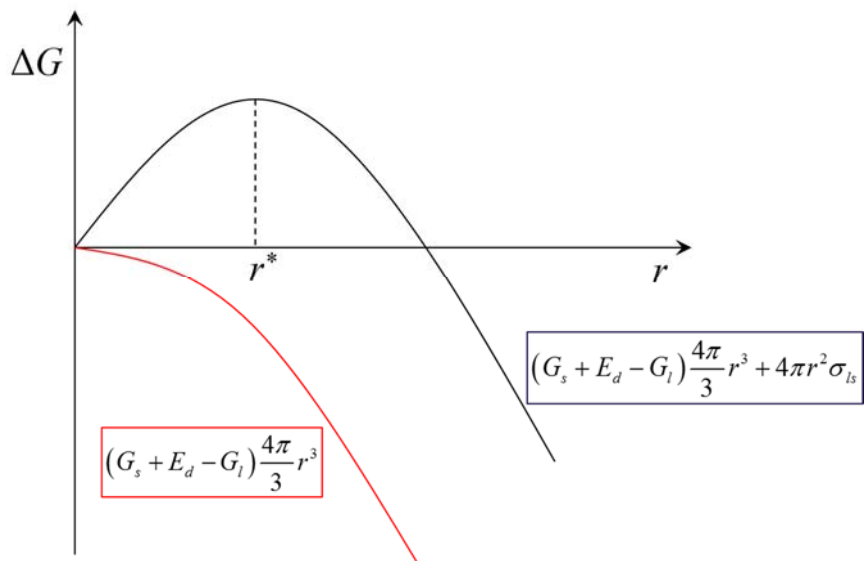


Figure 4. Gibbs free energy difference  $\Delta G$  versus radius  $r$  of solid nucleus in liquid-solid phase transition: black curve, critical radius  $r^*$  and Gibbs free energy difference in black rectangular denote the results from classical theory, while red curve and Gibbs free energy difference in red rectangular is the result from our theory.